Environ. Sci. Technol. **2002**, *36,* 5100−5105

Disaggregation Kinetics of a Peat Humic Acid: Mechanism and pH Effects

MARCELO J. AVENA[†] AND KEVIN J. WILKINSON*[,‡]

CABE (Analytical and Biophysical Environmental Chemistry), University of Geneva, Sciences II, 30 Quai E. Ansermet, CH-1211, Geneva 4, Switzerland, and INFIQC, Departamento de Fisicoquímica, Facultad de Ciencias Químicas, Universidad Nacional de Córdoba, Ciudad Universitaria, 5000 Córdoba, Argentina

Fluorescence correlation spectroscopy was used to study the disaggregation kinetics of a peat humic acid (PPHA) at several pH. FCS measures diffusion coefficients of fluorescent molecules and aggregates, thus allowing for the determination of disaggregation rates with a temporal resolution of seconds to minutes. Disaggregation was initiated by dilution of a peat concentrate consisting of a mixture containing 80% large aggregates (average hydrodynamic radius, r_H, of about 300 nm) and free monomers (average r_H of about 1 nm). Upon dilution at different pH values, aggregate size decreased, and the proportion of free monomers in solution increased until complete disaggregation occurred. The mechanism appeared to involve the release of monomers from the surface of the aggregates. The pH markedly affected the disaggregation rate. Complete disaggregation took 1 month at pH 3.6, took less than 1 h at pH 5.6, and was extremely rapid in alkaline solutions. The results suggested that at least two processes were operating in parallel with the overall rate being the sum of both processes. At pH higher than 4.5, the disaggregation rate increased more than 3 orders of magnitude per pH unit increase. For concentrations lower than 30 mg L^{-1}, the equilibrium condition for the PPHA was complete disaggregation even for a pH as low as 3.6.

Introduction

Humic substances (HS) are very active in binding ions, organic molecules, and mineral surfaces and are thereby potentially important to soil structure, soil fertility, and transport of pollutants in natural waters. HS influence soil and water properties through their participation in dynamic processes where their constituent molecules interact with other molecules or ions (complexation/decomplexation), with solid surfaces (adsorption/desorption), and among themselves (aggregation/disaggregation). These interactions are generally studied under conditions of assumed equilibrium or pseudo-equilibrium. In this case, ion binding curves (*1*−*3*), adsorption isotherms (*4*−*6*) or size data from fluorescence spectroscopy (*7*), and light scattering (*8*−*10*) or turbidimetry measurements (*11*) are usually presented. Studies examining the dynamics of the processes are undertaken much less frequently. Although there are a few reports examining the kinetics of binding between HS and fluorophores (*12*, *13*) or oxide surfaces (*14*), the interaction of the HS molecules among themselves (homoaggregation) has rarely been studied, and the special case of HS disaggregation kinetics seems to be absent from the literature.

The aggregation/disaggregation of HS is still a controversial topic (*15*) with two main points of view. One of them suggests that HS are associations of relatively small molecules held together by weak interaction forces including hydrophobic forces and hydrogen bonds (*16*). The other, more traditional viewpoint, proposes that HS are polymers that can assume a random coil conformation in solution (*17*). Although these conceptual models are still under discussion, supporters of both views agree that humic acids (HA) are able to form large macromolecular structures or aggregates in aqueous media at low pH or in the solid state, such as in soils (*15*−*17*). Indeed, HA "aggregates" have been detected by light scattering (*8*, *9*), turbidimetry (*11*), fluorescence spectroscopy (*12*), atomic force microscopy (*18*), and fluorescence correlation spectroscopy (*19*) in line with predictions of molecular mechanics (*20*). The association of HA molecules is favored at high concentrations, high ionic strengths, and low pH and is postulated to be due to hydrogen bonding, cation bridging, and dipole−dipole and hydrophobic interactions (*15*−*17*, *20*). At low pH, protonation of the (mainly carboxylic) functional groups results in a decrease of the electrostatic repulsion among the HA molecules, increasing the probability of aggregation.

The dynamics of HA aggregation/disaggregation is likely an important process controlling the transport and fate of pollutants. Aggregating molecules could trap inorganic or organic contaminants and thus protect them from being degraded or neutralized. Under various conditions, the aggregate structure could open, thereby releasing the pollutant in its active form. The molecular mechanisms of these processes are not known.

The goal of this paper is therefore to study the disaggregation kinetics of a HA by investigating the process at different pH using fluorescence correlation spectroscopy (FCS). A purified peat HA (PPHA) was employed in the study (*21*) since a general consensus exists that it forms aggregates even though no agreement is currently available on the aggregate size or stability. For example, using dynamic light scattering and voltammetry, Pinheiro et al. (*9*, *22*) observed large (diameter 30−185 nm) PPHA aggregates. They showed that an increase in pH led to a decrease in aggregate size whereas a decrease in pH led to further aggregation, coagulation, and precipitation. Milne et al. (*21*) postulated that aggregation/disaggregation was occurring in highly concentrated PPHA solutions in order to explain the hysteresis of their proton adsorption curves. Their titration data indicated that disaggregation was occurring with an increase in solution pH whereas very slow reaggregation was postulated when the pH was lowered to 4. They also determined H^+ consumption during PPHA aggregation. Finally, Balnois et al. (*18*) observed PPHA aggregates using atomic force microscopy (AFM). Large numbers of aggregates were documented at pH 3.2; fewer were observed at pH 5.2, while no aggregates were detected at neutral and basic pH.

Materials and Methods

A PPHA solution was kindly provided by D. G. Kinniburgh. It was isolated from an Irish peat using a slightly modified IHSS (International Humic Substances Society) procedure (*23*, *24*) including extensive dialysis (6 months, molecular

* Corresponding author phone: (41 22) 702 6051; fax: (41 22) 702 6069; e-mail: Kevin.Wilkinson@cabe.unige.ch.

[†] University of Córdoba.

[‡] University of Geneva.

10.1021/es025582u CCC: $22.00
Published on Web 10/23/2002

weight cutoff of 12 000−14 000). The stock solution had a concentration of 5.28 g L^{-1}, a pH of 3.2, an ash content of 0.2%, and an elemental composition of C 52.07%, H 5.07%, N 2.37%, S 0.57%, and O 39.93%. The PPHA was never lyophilized and was stored in the dark at 5 °C until use. Solid-state ^{13}C NMR (*21*) demonstrated that the PPHA contained a range of aliphatic and aromatic structures that were farily typical of a peat humic acid. Extensive characterization of the proton and cation binding properties of the PPHA can be found in the literature (*2*, *21*). Light scattering (*9*), viscometry (*25*), atomic force microscopy (*18*), and ^{13}C NMR data (*21*) have also been reported by several authors for this sample. A weight average molar mass of 23 000, as measured by equilibrium UV-scanning utracentrifugation in 1 M NaCl solutions, was reported by Milne et al. (*21*), although they indicated that the value was likely biased by the presence of aggregates and hence overestimated the molar mass of the PPHA.

In this paper, the disaggregation process was followed by FCS. Briefly, a 488-nm excitation laser light is focused into the HA solution using confocal optics. In this way, a volume element (confocal volume) of 0.5−1 μm^3 is illuminated. Temporary fluctuations in the fluorescence intensity in the confocal volume can be attributed to the translational diffusion of the naturally fluorescent HA molecules. Variations in the fluorescence intensity are analyzed using an autocorrelation function that allows the determination of both the concentration and the diffusion coefficient (via diffusion times) of the HA. The advantages and limitations of the FCS technique for studies of the diffusion coefficients of HA have been discussed elsewhere (*19*, *26*), and excellent agreement has been obtained with other relatively nonperturbing and nonfluorescence-based techniques such as NMR spectrometry, flow-field flow fractionation, and atomic force microscopy (*27*).

Under the assumption of a compact, spherical particle (*18*), the hydrodynamic radius (r_H) of the fluorescent entities can be calculated from the Stokes−Einstein equation:

$$r_H = \frac{kT}{6\pi\eta D} \quad (1)$$

where k is the Boltzmann constant, T is the absolute temperature, η is the solution viscosity, and D is the diffusion coefficient determined from FCS. The FCS system was calibrated by using Rhodamine 6G (R6G, Molecular Probes), which has a known diffusion coefficient of 2.8×10^{-10} m^2 s^{-1} (*28*). The pH was measured with a Metrohm combination glass electrode and a Metrohm E 603 pH meter. All chemicals were analytical grade. Demineralized (R > 18 MΩ·cm^{-1}), UV-irradiated water (TOC < 5 μg of C L^{-1}) was used throughout. All experiments were performed at 25 °C.

Disaggregation experiments were initiated by diluting the stock solution to a final concentration of 30 mg L^{-1} PPHA. The experimental solutions were prepared in one of two ways: (i) in 5×10^{-3} M NaCl solutions of different pH (adjusted with NaOH or HCl) or (ii) in 5×10^{-3} M "non-complexing" monovalent buffer solutions (*29*) for comparison (Table 1). Although the use of buffers can be problematic because of their potential to interact with the HA (*30*−*32*) and thus influence HA conformational structure, control of the pH was necessary, especially at the higher pH values (i.e., pH > 5) where the buffering capacity of the PPHA was weak. The use of overlapping pH conditions among buffered and nonbuffered solutions was employed in order to distinguish pH from buffer effects.

The disaggregation process was followed by measuring the diffusion times and the fractions of aggregated and disaggregated components as a function of time. At low pH, the disaggregation rate was low, and a complete experiment took several days. Under these conditions, each data point was determined as the mean of at least eight replicate measurements, each with a run time of 200 s. At higher pH values, rates were higher, and complete disaggregation took only several minutes. In this case, each data point represents an individual measurement with a run time of 30 s. Although the latter method has more error than the first, it allowed for the measurement of faster kinetics.

TABLE 1. Values of Disaggregation Rate, R_s (nm/day), for the PPHA at Each pH Studied[a]

pH	R_s	electrolyte	pH	R_s	electrolyte
3.60	2.9	NaCl	5.05	1 500	acetic/acetate
3.65	3.3	acetic/acetate	5.24	450	acetic/acetate
3.75	4.5	NaCl	5.31	4 500	malonic/malonate
3.90	5.4	acetic/acetate	5.31	5 400	malonic/malonate
4.24	6	NaCl	5.60	5 400	HMES/NaMES
4.32	6.9	acetic/acetate	5.60	6 700	HMES/NaMES
4.65	11.4	acetic/acetate	5.65	33 000	malonic/malonate
4.81	39	acetic/acetate	5.65	39 000	malonic/malonate
4.90	60	NaCl			

[a] In each case, experiments were performed at an ionic strength of 0.005 M. Where indicated, ionic strength corresponded to pH-buffered solutions. HMES and NaMES are the weak acid and sodium salt, respectively, of 2-(*N*-morpholino)ethanesulfonic acid.

Model and Data Analysis

A simple model was used to analyze the experimental results. In this model, it is assumed that the stock PPHA solution consists of a mixture of free (monomers) and associated molecules (aggregates). Both the monomers and the aggregates are assumed to be spherical. This is a reasonable first approximation given the available AFM images (*18*, *33*), and data indicating that the fractal dimensions of aggregates formed by reversible aggregation are larger than expected (*34*) as compared to those formed by irreversible aggregation (*35*). It is also assumed that the disaggregation process occurs through the release of monomers from the surface of the aggregates and that the probability of detachment is equal at any point on the surface. This implies that the number of aggregates does not change as disaggregation proceeds, rather aggregate size is reduced to give spheres of smaller and smaller radii. In this case, the reaction rate is predicted to be proportional to the surface area of the reacting material, and the overall reaction rate should decrease continuously in time because of a decrease in the surface area as the reaction progresses (*36*, *37*). This "attrition mechanism" is one of simplest explanations of the disaggregation process. In colloid science, other mechanisms such as attrition through the release of small fragments of several monomers, breaking of aggregates into smaller aggregates, or even a disintegration of the aggregates to produce only monomers are also known to take place (*38*, *39*).

Note that other disaggregation mechanisms could have been proposed. The attrition mechanism used here was selected because of its simplicity and because it seemed reasonable as a first approximation of the HA disaggregation process since surface-bound monomers should be detached quite easily with respect to monomers in the inner region of the aggregate. Indeed, breaking the few bonds required to remove a single surface-bound monomer is much easier than breaking the large number of bonds that a monomer has established with its neighbors in the inner region of the aggregate. Furthermore, it is also easier than the breaking of bonds required in order to divide a large aggregate into two or more pieces. Nonetheless, if there is a marked heterogeneity among the aggregates, it is possible that bond strengths change from one aggregate to another. In the limiting case, disaggregation could take place one aggregate

at a time, i.e., one aggregate would be completely disaggregated before the next begins to disaggregate (sequential disaggreation mechanism). Although this is an unlikely mechanism for HS, it will be used for comparison.

The state of aggregation or disaggregation of a system can be determined if the proportion of monomers that are present as free monomers, X, is known. It can be defined as

$$X = \frac{c_m}{c_{m,t}} \tag{2}$$

where c_m is the concentration of free monomers and $c_{m,t}$ is the total concentration of monomers (free monomers plus monomers forming the aggregates). The values of X range between 0 (complete aggregation) and 1 (complete disaggregation). The value of X at the beginning of a disaggregation process is denoted by X_0, and the change in X with time can be used as an estimation of the dissagregation rate.

Only a small fraction of HA molecules are fluorescent (*40*). Therefore, a completely dissagregated sample contains a large number of monomers that do not fluoresce. When aggregates are formed, especially very large aggregates containing hundreds or thousands of monomers, it is highly likely that each aggregate will have fluorescent entities that will act as a labeling agent for the aggregate. In a solution composed of very large aggregates and small monomers, FCS will detect only a fraction of the free monomers but most (if not all) of the aggregates. According to this reasoning, several equations, depending on the concentration of fluorescent entities, can be developed in order to calculate X.

The total concentration of fluorescent particles, c_p^f, in a HS solution is defined as

$$c_p^f = c_m^f + c_a \tag{3}$$

where c_m^f is the concentration of free monomers that fluoresce (number per unit volume) and c_a is the concentration of aggregates (number of aggregates per unit volume); all aggregates are assumed to be fluorescent. Note that c_m corresponds to all of the free monomers whereas c_m^f represents the free monomers that are fluorescent. The fraction of fluorescent particles found as monomers, X_m^f, and the fraction of particles that are found as aggregates, X_a, are given by

$$X_m^f = \frac{c_m^f}{c_p^f} \tag{4}$$

$$X_a = \frac{c_a}{c_p^f} \tag{5}$$

The values of c_p^f, X_m^f, and X_a together with the diffusion coefficients of the fluorescent monomers and aggregates are obtained directly from the fit of the autocorrelation function. c_m^f can be related to the concentration of free monomers by

$$\gamma_m^f = \frac{c_m^f}{c_m} \tag{6}$$

where γ_m^f is the proportion of monomers that fluoresce. The total concentration of monomers $c_{m,t}$ is constant in any given disaggregation experiment and is defined as the sum of free monomers and the monomers contained in aggregates. It can be obtained either by measuring c_p^f in a completely disaggregated solution or by performing a disaggregation experiment and extrapolating the corresponding c_p^f versus X_m^f curve to $X_m^f = 1$ (no aggregates present). Under those conditions, all fluorescent particles are free monomers ($c_p^f = c_m^f$), and thus $c_{m,t}$ can be calculated from a measured value of γ_m^f:

$$c_{m,t} = \frac{(c_p^f)_1}{\gamma_m^f} \tag{7}$$

where $(c_p^f)_1$ represents the concentration of fluorescent particles when $X_m^f = 1$.

Combining eqs 2, 4, 6, and 7:

$$X = \frac{X_m^f c_p^f}{(c_p^f)_1} \tag{8}$$

so that X can be related to measurable parameters obtained from the FCS measurement.

The degree of progress of the reaction, α, can be defined as

$$\alpha = \frac{X - X_0}{1 - X_0} \tag{9}$$

which indicates that $\alpha = 0$ at the beginning of the experiment and $\alpha = 1$ for complete disaggregation. The use of α allows for the direct application of the equations describing the attrition mechanism (*36*):

$$(1 - \alpha)^{1/3} = 1 - \frac{R_s}{r_{a,0}}t \tag{10}$$

where t is the reaction time, $r_{a,0}$ is the initial radius of the aggregate, and R_s (distance/time units) is the rate at which the radius of hypothetical spherical aggregate is decreasing (*36*). The fraction X can be plotted against time following combination of eqs 9 and 10:

$$X = X_0 + (1 - X_0)\left(1 - \left(1 - \frac{R_s}{r_{a,0}}t\right)^3\right) \tag{11}$$

In the other limiting case, the "sequential disaggregation" mechanism, aggregate number would decrease but the average aggregate size would not change significantly during the disaggregation process. In this case, there would be a predicted exponential dependence of α on t:

$$\alpha = 1 - e^{-kt} \tag{12}$$

where k is a constant. Combination of eqs 9 and 12 results in the X versus t dependence:

$$X = 1 - (1 - X_0)e^{-kt} \tag{13}$$

In reality, it is most likely that the disaggregation mechanism is somewhere between these two extreme cases, i.e., removal of a single monomer versus removal of a monomer cluster. These two limiting cases are therefore presented as a framework in which to discuss the observed results. Even more complicated exponential or power functions of t could be obtained by assuming that the aggregates are heterogeneous in size and produce fragments with a given size distribution (*38*). Although these mathematical treatments are out of the scope of this paper, they do not modify the conclusions given below.

Results and Discussion

FCS autocorrelation curves for a 30 mg L^{-1} PPHA solution at pH 4.9 and 5×10^{-3} M NaCl are given in Figure 1. The data

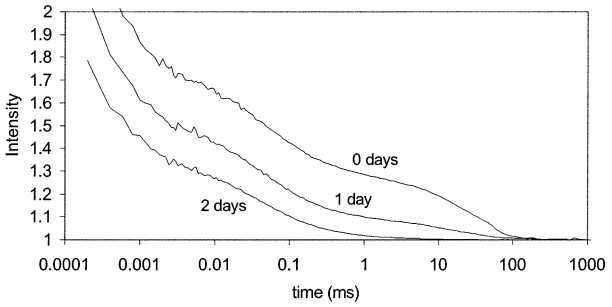

FIGURE 1. Autocorrelation curves obtained for a 30 mg L^{-1} PPHA solution at pH 4.90. The time shown on each curve corresponds to the time elapsed since initiation of the disaggregation process. I = 0.005 M, T = 25 °C.

were accumulated 0, 1, and 2 days after preparation of the solution from the stock PPHA. The curve at $t = 0$ has two inflection points corresponding to diffusion times on the order of 0.04 and 14 ms. This reveals the presence of at least two populations of fluorescent entities having two very different diffusion coefficients. Diffusion times around 14 ms (standard deviation, SD = 3 ms) corresponded to entities with $D \sim 7 \times 10^{-13}$ m^2 s^{-1} ($r_H \sim 300$ nm). Diffusion times around 0.04 ms (SD = 0.002 ms) corresponded to entities with $D \sim 2.5 \times 10^{-10}$ m^2 s^{-1} ($r_H \sim 1$ nm). The size of the small entities coincides with prior equilibrium AFM observations of the PPHA macromolecules at neutral pH values (*18*). The molar mass (M_w) of the monomer can be estimated to be around 1370 g mol^{-1} using the following empirical equation (*41*):

$$r_H = 0.027\sqrt{M_w} \quad (14)$$

where r_H is expressed in nanometers. This population is assumed to represent the monomers whereas the larger entities with small D corresponded to the aggregates. The size of the PPHA aggregates is on the order of the sizes reported by photon correlation spectroscopy and voltametry (*9*, *22*).

Analysis of the autocorrelation curves presented in Figure 1 indicated a total monomer concentration of 1×10^{-7} M. This concentration is significantly less than the estimation of 2.18×10^{-5} M obtained by dividing the known concentration employed (0.03 g L^{-1}) by the estimated value of the molecular weight (1370 g mol^{-1}). This indicated that $\gamma_m^f = 0.0045$, that is, only a small fraction (0.45%) of the molecules present in the solution were fluorescent at the excitation wavelength employed here (488 nm) in agreement with previous work (*19*, *40*). While such a small proportion of fluorescent humic molecules might bring into question whether the FCS technique can be representative of the entire population of humic molecules, the point is likely moot here. Experiments were designed to determine disaggregation rates of large aggregates that could be assumed to be fluorescent since they contained, on average, 10^6 individual humic molecules (based on the assumption of compact spheres). In addition, previous experiments (*42*) in which HS fractions separated by capillary electrophoresis demonstrated similar relative signals using fluorescence (325, 454, 488, and 514 nm) and absorbance (200 nm) detection suggested that the fluorescent fraction of the HS was fairly representative of the humic population as a whole.

Further analysis of the autocorrelation curves indicated that X increased from 0.25 (day 0) to 0.54 (day 1) to 0.86 after 2 days. The average diffusion coefficient of the monomers remained constant within experimental error, whereas that of the aggregates increased 2−3-fold (equivalent to a 2−3-fold decrease in radius) over 2 days. No evidence of a third component of intermediate size was found in any case. The results are clear evidence that disaggregation is occurring.

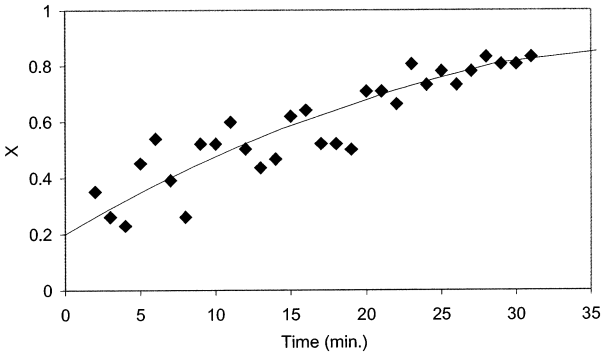

FIGURE 2. Fraction of monomers as a function of time obtained at pH 5.6 in a 0.005 M HMES/NaMES buffer. The solid line is predicted from eq 11 using R_s data given in Table 1 and $r_{a,0}$ = 300 nm.

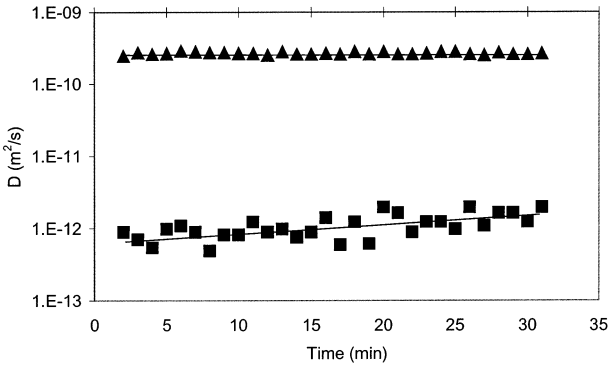

FIGURE 3. Evolution of the diffusion coefficients, D, as a function of time for aggregates (squares) and monomers (triangles) obtained at pH 5.6 in a 0.005 M HMES/NaMES buffer for a PPHA concentration of 30 mg L^{-1}.

At pH 5.6, disaggregation was much faster than at pH 4.9 (Figure 2). Only 30 min was necessary to reach $X = 0.83$, and although not shown here, disaggregation was complete in a little over 1 h. As was seen at pH 4.9, no significant variation was observed for the diffusion coefficients of the monomers ($D \sim 2.5 \times 10^{-10}$ m^2 s^{-1}; Figure 3). On the other hand, the measured diffusion coefficient for the aggregates changed from $D \sim 7 \times 10^{-13}$ to $D \sim 1.6 \times 10^{-12}$ m^2 s^{-1}.

For all studied solutions, X_0 was between 0.20 and 0.25, a value that is believed to represent the initial state of aggregation of the stock PPHA solution (Figure 4). Furthermore, as seen above, pH was a major parameter controlling disaggregation rate. Disaggregation was slow at pH 3.65 where it took more than 1 month to reach $X = 0.90$. At higher pH, the process was much faster. Above pH ≥ 6.3, aggregates were no longer detected 10 min following dilution. In Figure 4, the experimental points are shown together with the theoretical predictions of eq 11. A similar behavior was observed in unbuffered solutions (Table 1).

A good fit of the monomer fraction versus time curves was also obtained using eq 13 (Figure 4). In fact, the scatter of the experimental data does not allow us to give precedence to either of the mechanisms suggested by eqs 11 or 13. Nonetheless, the observation of decreasing aggregate size with no evidence of an independent third population of aggregates in an intermediate size range supports the attrition mechanism. The change in D from 7×10^{-13} to about 1.6×10^{-12} m^2 s^{-1} implies a 55% decrease in radius (eq 1) and a 90% decrease in volume for a spherical aggregate. The observed volume reduction is sufficient to explain the increase in X during disaggregation, also in support of the attrition mechanism.

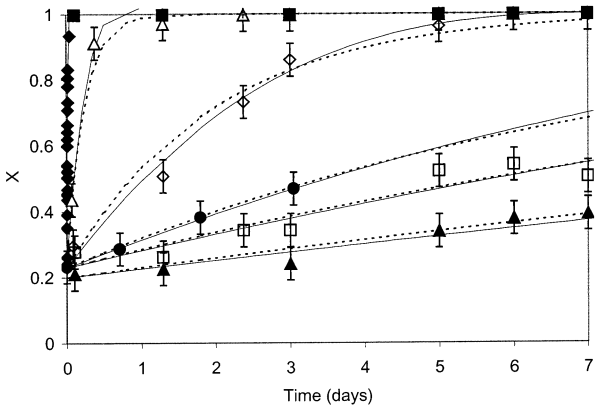

FIGURE 4. Effects of pH on the disaggregation kinetics of the PPHA. Measurements performed in 0.005 M buffer solutions at pH 3.65 (solid triangles), 4.32 (open squares), 4.65 (solid circles), 4.81 (open diamonds), 5.24 (open triangles), 5.6 (solid diamonds), and 6.28 (solid squares). Solid lines are predictions using eq 11 and R_s values given in Table 1 and $r_{a,0} = 300$ nm. Dashed lines are predictions using eq 13 and the following k values (obtained by curve fitting; day^{-1}): 0.046 (pH 3.65), 0.09 (pH 4.32), 0.15 (pH 4.65), 0.6 (pH 4.81), 5 (pH 5.24), 75 (pH 5.6).

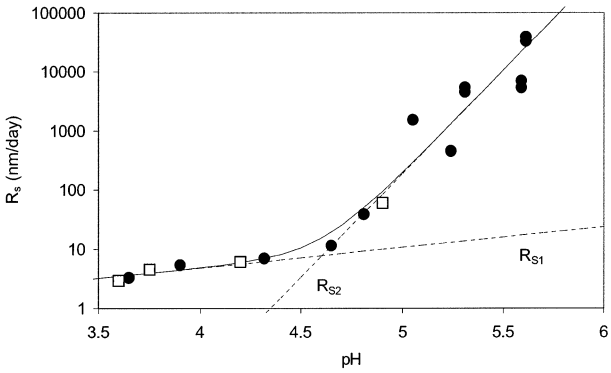

FIGURE 5. Effect of pH on R_s. Measurements performed in either 0.005 M NaCl (squares) or 0.005 M buffered (circles) solutions. Dashed lines correspond to R_{s1} and R_{s2}, and the solid line corresponds to R_s according to eq 15. $k_1 = 0.19$ nm/day, $k_2 = 6 \times 10^{-16}$ nm/day, $n = -0.35$, and $m = -3.5$.

R_s increased by more than 3 orders of magnitude from pH 3.6 to pH 5.6 (Figure 5). Similar variations with pH were obtained by plotting k (eq 13) as a function of pH or even initial disaggregation rates, $(dX/dt)_{t=0}$, versus pH. A good agreement with the data suggested that the pH dependence of the data could be well-established although the *attrition* and *sequential disaggregation* mechanisms could not be discriminated by model fits. The nonlinear behavior observed for all models was clear evidence that a single reaction did not predominate at all pH. Indeed, such pH effects can only be explained if at least two processes are operating in parallel, with the overall rate reflecting contributions from both processes. In this case, the rate law can be expressed as

$$R_s = R_{s1} + R_{s2} = k_1[H^+]^n + k_2[H^+]^m \qquad (15)$$

where R_{s1} and R_{s2} are the respective rates of the two processes, k_1 and k_2 are rate constants, $[H^+]$ is the proton concentration in the solution, and n and m are reaction orders for the protons. Each of the lines given in Figure 5 corresponds to one of the two rates described by $\log R_{s1} = \log k_1 + n \log[H^+]$ or $\log R_{s2} = \log k_2 + m \log[H^+]$.

For the dissolution of metal oxides, where the detachment of the metal ion is the rate-determining step, the proton reaction order indicates the number of fast protonation (positive order) or deprotonation (negative order) steps that occur prior to the detachment of the metal ion (*43*). By analogy, if the detachment of a PPHA molecule from the aggregate is the rate-determining step, negative values of n and m would suggest an initial fast deprotonation. Best fit values of eq 15 gave $k_1 = 0.19$ nm day^{-1}, $k_2 = 6 \times 10^{-16}$ nm day^{-1}, $n = -0.35$, and $m = -3.5$. These data were supported by that of Milne et al. (*21*), who demonstrated that at pH 4 there was a difference in proton consumption between aggregated and disaggregated PPHA of about 0.5 mol of protons/kg of humic acid (*21*). For an average M_w of 1370, this result suggests that about 0.36 mol of protons would be released/mol of PPHA during the disaggregation process. In light of the similarity between the value of n (−0.35) and the number of protons consumed per PPHA molecule during disaggregation (0.36), R_{s1} could, in principle, be assigned to this process. It is possible to speculate that the process is related to the breaking of hydrogen bonds holding the PPHA molecules together in an aggregate. The release of protons involved in these bonds could leave the molecules more susceptible to detachment.

At pH values corresponding approximately to pH > pK_a of the carboxylic acid functional groups of the PPHA (*1*), the disaggregation rate increased significantly. Since deprotonation will increase electrostatic repulsion among the molecules, the increase in rate is likely due to the development of a significant negative charge of the monomers because of deprotonation of the (mainly carboxylic) functional groups. If the detachment step is rate determining, this result suggests that an average of 3.5 ($m = -3.5$) protons should be released from ionizable groups prior to the detachment of the PPHA monomers. This observation is also coherent with the known carboxyl content of the PPHA of ca. 4.5 COOH per monomer (*21*).

The results described above may have significant importance for environmental systems because they imply that at low pH HS could temporarily trap, protect, and transport organic molecules, pesticides, metal ions, and other substances in large aggregates. At slightly higher pH, disaggregation could lead to the release of the molecules. The capacity of the HS to aggregate (or disaggregate) will depend on the size of the monomers, their hydrophobicity, and their capacity to establish weak hydrogen or hydrophobic bonds among the monomers. Indeed, other experiments examining more hydrophilic aquatic fulvic acids (data not shown) were unable to produce aggregates under similar conditions to those observed here for the PPHA. On the other hand, the PPHA studied in this work will form large aggregates at high HS concentrations but will quickly disaggregate upon dilution in all but very acid waters. For typical HS concentrations in natural freshwaters (<30 mg L^{-1}), the equilibrium condition for the PPHA is complete disaggregation even at pH 3.6. Therefore, this is a potentially important mechanism for the transport and release of hydrophobic pollutants from areas of high HS concentration, such as soils, to water bodies with corresponding lower concentrations, including rivers or lakes.

Acknowledgments

Funding for this work was provided by the Swiss National Foundation Grants 2000-050529.971 and 2000-61648.00. M.J.A. thanks CONICET and FUNDACION ANTORCHAS for their support. Helpful comments and suggestions by M. Borkovec, J. Buffle, and K. Startchev are greatly appreciated. We thank D. Kinniburgh for providing the purified peat HA (PPHA).

Literature Cited

(1) Avena, M. J.; Koopal, L. K.; van Riemsdijk, W. H. *J. Colloid Interface Sci.* **1999**, *217*, 37.

(2) Kinniburgh, D. G.; van Riemsdijk, W. H.; Koopal, L. K.; Borkovec, M.; Benedetti, M. F.; Avena, M. J. *Colloids Surf. A* **1999**, *151*, 147.
(3) Brown, G. K.; Cabaniss, S. E.; MacCarthy, P. *Anal. Chim. Acta* **1999**, *402*, 183.
(4) Namjesnik-Dejanovic, K.; Maurice, P. A.; Aiken, G. R.; Cabaniss, S.; Chin, J.-P.; Pullin, M. J. *Soil Sci.* **2000**, *165*, 545.
(5) Au, K. K.; Penisson, A. C.; Yang, S.; O'Melia, C. *Geochim. Cosmochim. Acta* **1999**, *63*, 2903.
(6) Zhou, J. L.; Rowland, S.; Mantoura, F. C.; Braven, J. *Water Res.* **1994**, *28*, 571.
(7) Jones, G., II.; Indig, G. L. *New J. Chem.* **1996**, *20*, 221.
(8) Tombacz, E.; Rice, J. E.; Ren, S. Z. *Models Chem.* **1997**, *134*, 877.
(9) Pinheiro, J. P.; Mota, A. M.; d'Oliveira, J. M. R.; Martinho, J. M. G. *Anal. Chim. Acta* **1996**, *329*, 15.
(10) Manning, T. J.; Bennet, T.; Milton, D. *Sci. Total Environ.* **2000**, *257*, 171.
(11) Senesi, N.; Rizzi, F. R.; Dellino, P.; Acquafredda, P. *Colloids Surf. A* **1997**, *127*, 57.
(12) Engebretson, R. R.; Von Wandruszka, R. *Environ. Sci. Technol.* **1998**, *32*, 488.
(13) Weber, E. J.; Spidle, D. L.; Thorn; K. A. *Environ. Sci. Technol.* **1996**, *30*, 2755.
(14) Avena, M. J.; Koopal, L. K. *Environ. Sci. Technol.* **1999**, *33*, 2739.
(15) Clapp, C. E.; Hayes, M. H. B. *Soil Sci.* **1999**, *164*, 777.
(16) Piccolo, A. *Soil Sci.* **2001**, *166*, 810.
(17) Swift, R. S. *Soil Sci.* **1999**, *164*, 790.
(18) Balnois, E.; Wilkinson, K. J.; Lead, J. R.; Buffle, J. *Environ. Sci. Technol.* **1999**, *33*, 3911.
(19) Lead, J. R.; Wilkinson, K. J.; Starchev, K.; Canonica, S.; Buffle, J. *Environ. Sci. Technol.* **2000**, *34*, 1365.
(20) Schulten, H. R.; Leinweber, P. *Biol. Fertil. Soils* **2000**, *30*, 399.
(21) Milne, C. J.; Kinniburgh, D. G.; De Wit, J. C. M.; van Riemdijk, W. H.; Koopal, L. K. *Geochim. Cosmochim. Acta* **1995**, *59*, 1101.
(22) Pinheiro, J. P.; Mota, A. M.; Simoes Goncalves, M. L. S.; van Leeuwen, H. P. *Colloids Surf. A* **1998**, *137*, 165.
(23) Thurman, E. M.; Malcolm, R. L. *Environ. Sci. Technol.* **1981**, *15*, 463.
(24) Reid, P. M.; Wilkinson, A. E.; Tipping, E.; Jones, M. N. *Geochim. Cosmochim. Acta* **1990**, *54*, 131.
(25) Avena, M. J.; Vermeer, A. W. P.; Koopal, L. K. *Colloids Surf. A* **1999**, *151*, 213.
(26) Starchev, K.; Wilkinson, K. J.; Buffle, J. In *Fluorescence Correlation Spectroscopy*: *Theory and Applications*; Rigler, R., Elson, E. L., Eds.; Springer: Heidelberg, 2001; Chapter 12, pp 251−275.
(27) Lead, J.; Wilkinson, K. J.; Balnois, E.; Larive, C.; Cutak, B.; Assemi, S.; Beckett, R. *Environ. Sci. Technol.* **2000**, *34*, 3508.
(28) Elson, E. L.; Magde, D. *Biopolymers* **1974**, *13*, 1.
(29) Good N. E.; Winget, D.; Winter, W.; Connolly, T. N.; Izawa, S.; Singh, R. M. M. *Biochemistry* **1966**, *5*, 467.
(30) Piccolo, A.; Nardi, S.; Cancheri, G. *Eur. J. Soil Sci.* **1996**, *47*, 319.
(31) Cozzolino, A.; Conte, P.; Piccolo, A. *Soil Biol. Biochem.* **2001**, *33*, 563.
(32) Hosse, M.; Wilkinson, K. J. *Environ. Sci. Technol.* **2001**, *35*, 4301.
(33) Buffle, J.; Wilkinson, K. J.; Stoll, S.; Filella, M.; Zhang, J. *Environ. Sci. Technol.* **1998**, *32*, 2887.
(34) Fernandez-Nieves, A.; Fernandez-Barbero, A.; Vincent, B.; de las Nieves, F. J. *Langmuir* **2001**, *17*, 1841.
(35) Lin, M. Y.; Lindsay, H. M.; Weitz, D. A.; Ball, R. C.; Klein, R.; Meakin, P. *Nature* **1989**, *339*, 360.
(36) Harrison, L. G. In *Comprehensive Chemical Kinetics. The Theory of Kinetics*; Bamford, C. H., Tipper, C. F. H., Eds.; Elsevier: Amsterdam; 1969; p 377.
(37) Avena, M. J.; De Pauli, C. P. *Colloids Surf. A* **1996**, *108*, 181.
(38) Stoll, S.; Pefferkorn, E. *J. Colloid Interface Sci.* **1992**, *152*, 61.
(39) Cheng, Z.; Redner, S. *Phys. Rev. Lett.* **1988**, *60*, 2450.
(40) Senesi, N. *Anal. Chim. Acta* **1990**, *232*, 77.
(41) Buffle, J. *Complexation Reactions in Aquatic Systems: An Analytical Approach*; Ellis Horwood Limited: Chichester, England, 1988.
(42) Lead, J. R.; Balnois, E.; Hosse, M.; Menghetti, R.; Wilkinson, K. J. *Environ. Int.* **1999**, *25*, 245.
(43) Stumm, W.; Morgan, J. J. *Aquatic Chemistry. Chemical Equilibria in Natural Waters*; Wiley-Interscience: New York, 1996.

Received for review February 13, 2002. Revised manuscript received July 29, 2002. Accepted September 20, 2002.

ES025582U